

Photochemistry of Iodopentaamminerhodium(III) in Zeolite Y

MICHAEL J. CAMARA and JACK H. LUNSFORD*

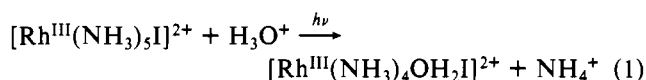
Received December 7, 1982

The photoaquation of iodopentaamminerhodium(III) in fully and partially hydrated zeolite Y was studied as a model reaction to explore the photochemistry of transition-metal complexes in zeolites. The reaction was followed via infrared spectroscopy by observing the production of the NH_4^+ ion. In the treatment of the data, several techniques were applied to account for scattering of light by the zeolite. Upon irradiation at 436 nm, the best values of quantum yield were 0.18 ± 0.03 in the hydrated zeolite and 0.13 ± 0.03 in the partially dehydrated zeolite at 25 °C. In aqueous solution the quantum yield increased slightly with ionic strength; at an ionic strength of 0.1 the quantum yield was 1.06 ± 0.08 . Steric hindrance, which results from the location of the complex relative to the walls of the zeolite cavity, may be responsible for the decrease in quantum yield. Light scattering, in addition to a decrease in quantum yield, results in the inefficient utilization of light for the photoaquation reaction in zeolites.

Introduction

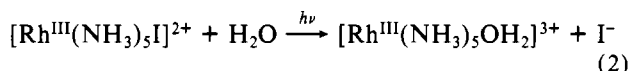
The intracrystalline cavities of zeolites provide a novel medium for carrying out inorganic chemistry. Numerous complexes have now been synthesized within these voids, and in some cases the catalytic role of complexes has been demonstrated.^{1,2} The photophysical properties of $\text{Ru}^{\text{II}}(\text{bpy})_3\text{-Y}$ and Cu-Y zeolites have been reported recently.^{3,4} In addition, the photoreduction of water has been achieved with an Ag-Y zeolite.⁵ No work has been carried out, however, that would allow one to compare a photochemical reaction in a zeolite with its counterpart in a more conventional solvent.

The objective of this research was not only to make such a comparison but also to explore several models for evaluating the quantum efficiency in a solid polycrystalline sample. The ligand-exchange photochemistry of iodopentaamminerhodium(III) was chosen for this study because the primary reaction



may be readily followed in a zeolite by observing the characteristic infrared band due to the ammonium ion. Diffuse-reflectance spectroscopy was also used to follow the photochemical reaction, although not under monochromatic conditions.

Kelly and Endicott^{6,7} have studied extensively the photo-reactions of $[\text{Rh}^{\text{III}}(\text{NH}_3)_5\text{I}]^{3+}$ in aqueous media and have found that the quantum efficiency for reaction 1 has a relatively constant value of $\phi_{\text{NH}_3} = 0.85 \pm 0.05$ over irradiation wavelengths from 385 to 470 nm at 25 °C, an ionic strength of 0.1, and a pH range of 1-3. At shorter wavelengths the quantum yields decrease and at 214 nm $\phi_{\text{NH}_3} = 0.41 \pm 0.02$. Reaction 1 is strongly favored over the I^- aquation reaction



which has a quantum yield of $\phi_{\text{I}} = 0.01$ at $\lambda_{\text{irrad}} = 385\text{-}420$ nm.

In the work to be described here $[\text{Rh}^{\text{III}}(\text{NH}_3)_5\text{I}]^{3+}$ complexes were exchanged into a NaH-Y zeolite, which was subsequently air dried and pressed into thin wafers. The photoaquation reaction takes place in the large cavities of the zeolite, which are approximately 13 Å in diameter. As a crude approximation, one might view each cavity as a microcontainer in which the zeolite lattice functions as the anion, but in reality the system is more complex since even in the hydrated state a significant fraction of the cations will be associated with the lattice in well-defined sites. This influences not only the effective pH and ionic strength of the "solution" in the cavities but also the rate of energy transfer between excited states of the complex and the lattice.

Experimental Section

Preparation of Reagents. Rhodium trichloride, obtained from Engelhard, was used to prepare the chloropentaammine complex according to the method of Addison et al.⁸ This complex was then used as a starting material for the preparation of $[\text{Rh}(\text{NH}_3)_5\text{I}](\text{ClO}_4)_2$. In our hands a modification of the method outlined by Jørgensen⁹ gave better yields and a higher purity material than the method of Bushnell et al.¹⁰ According to the method of Jørgensen, $[\text{Rh}(\text{NH}_3)_5\text{I}]_2$ was first prepared; this solid was then mixed with 6 M perchloric acid and stirred at 25 °C for 45 min. During this time the crystalline phase was always present. Under a red Kodak safelight the crystals were filtered and washed twice with aliquots of concentrated perchloric acid and twice with ethanol. The air-dried $[\text{Rh}(\text{NH}_3)_5\text{I}](\text{ClO}_4)_2$ product displayed absorption bands at 417 and 279 nm, which agreed with literature values of 416 and 278 nm.¹¹ The purity of the material was >95%.

The NaH-Y zeolite was prepared by adding 5 g of Na-Y zeolite (Linde lot no. 3365-94) to a rapidly stirring solution of acetic acid (4 L, 10^{-4} M) at 25 °C. After 12 h of stirring, more acetic acid was added slowly to return the pH to 4, and thereafter the pH of the slurry did not change. The zeolite was filtered, washed twice with 50-mL aliquots of water, and air-dried. The extent of exchange was deduced from the amount of acetic acid needed to maintain the solution at pH 4, and it was found that approximately 50% of the sodium ions had been replaced by protons. The crystalline integrity of the zeolite was verified by comparing the X-ray powder patterns before and after hydronium ion exchange.

The $[\text{Rh}^{\text{III}}(\text{NH}_3)_5\text{I}]^{2+}$ complex was exchanged into the NaH-Y zeolite by adding 0.568 g of the zeolite to a 700-mL solution of 3.1×10^{-4} M $[\text{Rh}(\text{NH}_3)_5\text{I}](\text{ClO}_4)_2$ in the dark. After 24 h, the zeolite was filtered, washed once with 50 mL of water, and dried. An analysis of the filtrate indicated that the zeolite contained 2.5×10^{-4} mol/g of 4.5 rhodium complexes per unit cell. This value corresponds to

- (1) Lunsford, J. H. *ACS Symp. Ser.* **1977**, No. 40, 473. Kellerman, R.; Klier, K. *Surf. Defect Prop. Solids* **1975**, 4, 1.
- (2) Iizuka, T.; Lunsford, J. H. *J. Am. Chem. Soc.* **1978**, 100, 6106.
- (3) DeWilde, W.; Peeters, G.; Lunsford, J. H. *J. Phys. Chem.* **1980**, 84, 2306.
- (4) Strome, D. H.; Klier, K. *J. Phys. Chem.* **1980**, 84, 981.
- (5) Jacobs, P. A.; Uytterhoeven, J. B.; Beyer, H. *J. Chem., Soc. Chem. Commun.* **1977**, 128.
- (6) Kelly, T. L.; Endicott, J. F. *J. Am. Chem. Soc.* **1972**, 94, 1797.
- (7) Kelly, T. L.; Endicott, J. F. *J. Phys. Chem.* **1972**, 76, 1937.

- (8) Addison, A. W.; Dawson, K.; Gillard, R. D.; Heaton, B. T.; Shaw, H. *J. Chem. Soc., Dalton Trans.* **1972**, 589.
- (9) Jørgensen, S. M. *J. Prakt. Chem.* **1883**, 27, 433.
- (10) Bushnell, G. W.; Lalor, G. C.; Moelwyn-Hughes, E. A. *J. Chem. Soc. A* **1966**, 717.
- (11) Jørgensen, C. K. *Acta Chem. Scand.* **1956**, 10, 500.

ca. 0.5 rhodium complex per large cavity. At this exchange level, there was a fivefold excess of hydronium ions in the zeolite.

Light Source and Calibration. A 100-W mercury vapor lamp (GE H100 A4/T) was coupled with a collimating lens and chemical filter solutions to isolate the 435.8-nm line. The filter solutions were contained in two cells, each 10 cm in length. The first solution was 1.09 M in NaNO_2 , and the second was 0.018 M in CuSO_4 and 2.7 M in NH_4OH .

The light intensity was determined by ferrioxalate actinometry. Iron and oxalate solutions were prepared in separate vessels and were photochemically inert until they were mixed and diluted to give a fresh actinometer solution. The intensity of the light source was constant during each run, provided 30 min or more was allotted for the lamp to stabilize. The light source was calibrated at the beginning of each experiment. In this study it is more convenient to treat the radiation as a flux and to report its intensity as einsteins $\text{cm}^{-2} \text{min}^{-1}$ rather than the usual units of einsteins $\text{L}^{-1} \text{min}^{-1}$.

Irradiation Experiments. Under darkroom conditions the exchanged zeolite was pressed into wafers that contained $\leq 5 \text{ mg/cm}^2$. This corresponds to a thickness of $\leq 40 \mu\text{m}$. The wafers (1 cm \times 2 cm) were placed in a Pyrex infrared cell that had KCl windows. A Beckman IR-9 infrared spectrophotometer was used in the experiments. After the background infrared spectrum was recorded between 1200 and 2000 cm^{-1} , the cell was rotated 90°, and the wafer was irradiated with the visible source for a preset time interval. At the end of this time, the cell was returned to its original position and the infrared spectrum was again recorded. The buildup of the ammonium ion band at 1455 cm^{-1} and the decrease in the coordinated ammonia band at 1335 cm^{-1} were observed.

The absolute amount of ammonium ions in three $\text{NaNH}_4\text{-Y}$ zeolites was determined by the Kjeldahl method. These zeolites were prepared by ion exchange of NaH-Y in NH_4Cl solutions of different concentrations, after which the material was filtered and dried. The zeolite samples were pressed into wafers of different thickness, and the infrared absorption spectrum was recorded between 1250 and 1650 cm^{-1} . The area of the band at 1455 cm^{-1} was determined and plotted as a function of the concentration of NH_4^+ in the zeolite, expressed as $\mu\text{mol cm}^{-2}$. When plotted in this manner, the data fell on a straight line that had an intercept of zero. This linear relationship was then used as a calibration curve to determine the amount of NH_4^+ per cm^2 of an unknown sample.

Irradiation studies also were carried out in aqueous solutions that were degassed by bubbling Cr^{II} -scrubbed nitrogen through them before and during the reaction. In a typical experiment a $6.3 \times 10^{-3} \text{ M}$ solution of $[\text{Rh}(\text{NH}_3)_5\text{I}](\text{ClO}_4)_2$ was adjusted to a pH of 3 with HClO_4 and an ionic strength of 0.1 with NaClO_4 . This solution was placed in a quartz cell and irradiated through a 1- cm^2 window. In this case, the photon flux was converted to the more conventional units of einsteins $\text{L}^{-1} \text{min}^{-1}$ and the solution equation

$$\phi = \frac{[\text{P}]}{I_0(1 - 10^{-\epsilon[\text{C}]})t} \quad (3)$$

was used to determine the quantum yield. Here [P] is the molar concentration of product, I_0 is the source intensity, ϵ and [C] are the molar extinction coefficient and the concentration of the absorber, and l is the cell thickness.

Diffuse-Reflectance Experiment. Diffuse-reflectance spectra, expressed as the Schuster-Kubelka-Munk remission function, were obtained for the zeolite with a Cary 14 spectrophotometer with a Type II integrating sphere. In this configuration the sample is irradiated with the full spectrum of the light source. The sample was in the form of a relatively thick wafer, and MgO was used as the reference. The scan rate was 60 nm/min over the range 340–700 nm; thus the sample received 6 min of irradiation during each scan.

Results

Diffuse-Reflectance Spectra. As indicated in Figure 1, the $[\text{Rh}^{\text{III}}(\text{NH}_3)_5\text{I}]^{2+}$ complex in zeolite Y exhibits a maximum in the diffuse-reflectance spectra at ca. 420 nm compared to a maximum at 416 nm in aqueous solution. As the sample was irradiated by the light source in the spectrophotometer, the band due to the reactant decreased in intensity and the spectrum of the $[\text{Rh}^{\text{III}}(\text{NH}_3)_4\text{OH}_2\text{I}]^{2+}$ product began to appear at 480 nm ($\lambda_{\text{soln}} = 485 \text{ nm}$). Isosbestic points at 365 and 450 nm indicate that only one reactant and one product were

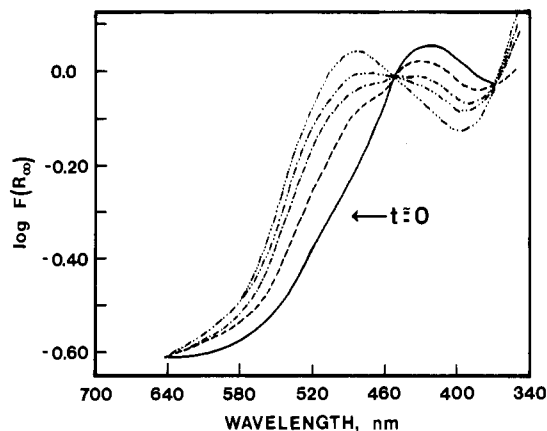


Figure 1. Diffuse reflectance spectra of $[\text{Rh}^{\text{III}}(\text{NH}_3)_5\text{I}]\text{-Y}$ zeolite following irradiation for various periods at 430 nm: —, $t \approx 0$; ---, $t = 6.7 \text{ min}$; ···, $t = 13 \text{ min}$; -·-·, $t = 19 \text{ min}$; ·-·-·, $t = 37 \text{ min}$.

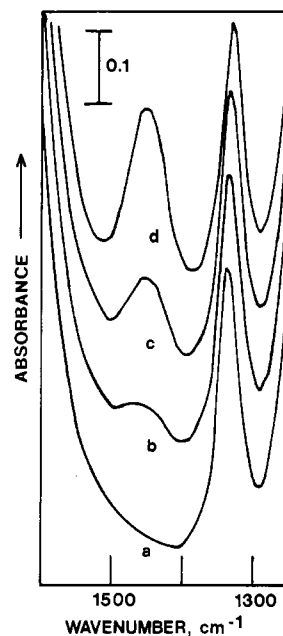


Figure 2. Infrared spectra of $[\text{Rh}^{\text{III}}(\text{NH}_3)_5\text{I}]\text{-Y}$ zeolite following irradiation for various periods: (a) $t = 0$; (b) $t = 50 \text{ min}$; (c) $t = 240 \text{ min}$; (d) $t = \infty$.

present during the photoaquation reaction.

Photochemical Reaction Profile in Zeolite Y. As the photoaquation of exchanged $[\text{Rh}^{\text{III}}(\text{NH}_3)_5\text{I}]^{2+}$ proceeded, the absorption band at 1450 cm^{-1} due to ammonium ions increased, as shown in Figure 2. The band at 1340 cm^{-1} is due to coordinated ammonia. Since the wafers could not be pressed in total darkness, a correction was made for the small amount of product that appeared in the infrared spectrum before the start of the irradiation. This correction usually amounted to less than 2% of the moles of reactant initially present. The increase in ammonium ion per cm^2 of external surface is plotted in Figure 3 for four different wafers. Wafers 1–3 were fully hydrated, but wafer 4 was partially dehydrated by keeping the sample under vacuum for 12 h at 25 °C. This treatment removed approximately 35% of the zeolite water, which decreased the available water molecules from about 50 per complex to 35 per complex. Extraction of the quantum yield from these data is described in the subsequent section.

Quantum Yield in Solution. For comparison purposes quantum yields were obtained in aqueous solution at two ionic strength levels and at a complex concentration of $6.5 \times 10^{-3} \text{ M}$. The concentration of ammonium ions varied in a linear manner with time of irradiation for small extents of conversion.

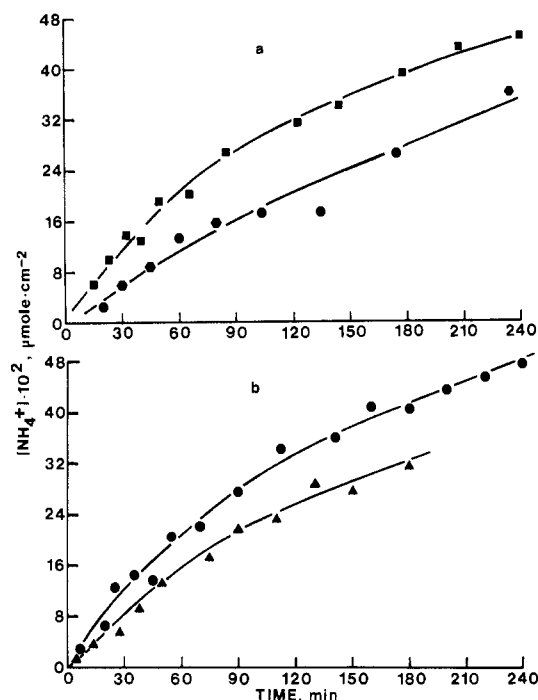


Figure 3. Variation of the NH_4^+ concentration as a function of irradiation period for four zeolite samples. The samples are designated by their thickness, expressed in mg/cm^2 : \blacksquare , 4.5; \bullet , 4.4; \blacktriangle , 3.1; \blacktriangle , 4.1.

The quantum yields, obtained by using eq 3, were $\phi = 0.52 \pm 0.05$ at $\mu = 0.020$ and $\phi = 1.06 \pm 0.08$ at $\mu = 0.10$. The latter value is only slightly greater than the value of $\phi = 0.87 \pm 0.07$ at $\mu = 0.10$ reported by Kelly and Endicott.⁶

Determination of Quantum Yield in the Solid Phase

Phenomena such as light scattering, reflection, and concentration gradients make the analysis of solid-state photochemical data much more complicated than that of liquid solutions. In this section several approaches will be taken to extract the quantum yields from the data of Figure 3.

Pseudo-Zero-Order Approach. In the first of these methods approximate quantum yields are obtained by assuming that the wafer does not transmit visible light and that it is partially transparent to infrared light. In addition we assume that only the reactant absorbs in the region of excitation and that the diffuse reflectance of the sample is the same over its entire apparent surface. In this case, where no visible light is transmitted, the incident light must be adsorbed or reflected. The fraction of the light initially absorbed by the reactant is given by

$$f_{\text{abs}} = 1 - R \quad (4)$$

where R is the measured reflectance of the sample. If the extent of the reaction is small, then f_{abs} may be considered a constant and the rate equation becomes

$$\frac{d[\text{P}]}{dt} = \phi(1 - R)I_0 \quad (5)$$

where I_0 signifies the light intensity in units of einsteins $\text{cm}^{-2} \text{min}^{-1}$. The integral form of this equation is

$$[\text{P}] = \phi(1 - R)I_0 t \quad (6)$$

from which ϕ may be determined.

The data of Figure 3 may be approximated by straight lines for the first 5 min of the reaction. The fraction of light absorbed ($1 - R$) was assumed to be constant during this time and was 0.50 at 430 nm as determined for a thick wafer containing the same loading of rhodium complex. The values of the quantum yields, ϕ , obtained by this method are listed in Table I. An estimated error of $\pm 10\%$ is primarily due to inaccuracy in determining the slope of the lines at low conversions.

First-Order Approach. In a second and more rigorous treatment developed by Simmons,¹² the rate of reaction of a thin layer of powder

Table I. Summary of Quantum Yields

thickness, mg/cm^2	environment	$10^{-7}k'$, $\text{cm}^2/\text{mol}^{-1}$	ϕ	ϕ_{av}
(A) Pseudo Zero Order				
3.1	air		0.20	} 0.22 ± 0.02
4.1	air		0.22	
4.5	air		0.25	
4.4	vac		0.17	
(B) First Order				
3.1	air		0.20	} 0.19 ± 0.02
4.1	air		0.19	
4.5	air		0.18	
4.4	vac		0.13	
(C) Exponential Decay				
3.1	air	0.30	0.15	} 0.15 ± 0.03
4.1	air	0.37	0.11	
4.5	air	0.40	0.19	
4.4	vac	0.20	0.10	
(D) Homogeneous, H_2O				
...	$\mu = 0.020$			0.52 ± 0.05
...	$\mu = 0.10$			1.06 ± 0.08
...	$\mu = 0.10$			0.87 ± 0.07^a

^a Reference 6.

can be easily applied to the present system. Consider a thin layer, one particle deep, of reactant C in the form of spherical particles having a rough surface. The incident radiation is both monochromatic and perpendicular to the surface. In each particle there are N mol of C; thus the rate of reaction may be described by

$$\frac{dN}{dt} = f\phi I\pi d^2/4 \quad (7)$$

where f is the fraction of light absorbed by the reactant and $I\pi d^2/4$ is the number of einsteins incident on the particle. The particle diameter is denoted by d and the concentration $[C]$ per unit area is given by

$$[C] = mN/Z \quad (8)$$

where m is the number of particles, each containing N mol, and Z is the surface area. Combining eq 7 and 8 yields the rate equation in terms of concentration:

$$\frac{d[C]}{dt} = mf\phi I\pi d^2/4Z \quad (9)$$

The fraction of light adsorbed (f) depends on factors such as external and internal reflection, which in turn are a function of the refractive index η . Treatment of this phenomenon by Simmons leads to the equation

$$\frac{d[C]}{dt} = \phi\epsilon\eta^2 I[C] \quad (10)$$

or in integral form

$$\frac{\ln([C]/[C]_0)}{t} = -\phi\eta^2\epsilon I_0 \quad (11)$$

A first-order plot of the data in Figure 3 gives reasonable good straight lines from which the quantum yield may be determined. Because I_0 is expressed as einsteins $\text{cm}^{-2} \text{min}^{-1}$, ϵ must have the units mol/cm^2 . By visually observing the light-scattering properties of a Y-type zeolite in several pure liquids, we determined the value of the refractive index to be 1.51, which is within the range of refractive indices of some naturally occurring zeolites.¹³ The value of ϵ was assumed to be the same as that found in aqueous solution. The resulting quantum yields obtained by this first-order approach are given in Table I.

Exponential Decay of Intensity. A semiempirical approach to the determination of quantum yields in solids has been developed by

(12) Simmons, E. L. *J. Phys. Chem.* **1974**, *78*, 1265.

(13) "Handbook of Chemistry and Physics", 35th ed.; Chemical Rubber Co.: Cleveland, OH, 1953; p 1409.

Spencer and Schmidt¹⁴ to account for the fact that the photoproduct may be formed near the surface and attenuate part or all of the incident radiation. The model also includes the effect of light scattering, which is of primary importance in this study.

A fundamental assumption of this model is that the intensity I transmitted through the solid decreased exponentially with thickness x as expressed by

$$I = I_0 e^{-kx} \quad (12)$$

The parameter k is an attenuation constant that represents a combination of absorption and scattering factors.

When the concentration of product $[\text{P}]$ is measured in mol cm^{-2} and the density of product in the solid ρ is in mol cm^{-3} , the rate of reaction can be described by

$$\frac{d[\text{P}]}{dt} = \frac{\rho dx}{dt} = \phi I = \phi I_0 e^{-kx} \quad (13)$$

With the assumption that the transmission through the entire wafer is zero and that the quantum yield is independent of x , eq 13 may be integrated and rearranged to give

$$[\text{P}] = \frac{1}{k'} \ln(1 + k'\phi I_0 t) \quad (14)$$

where $k' = k/\rho$. This equation was fitted to the data of Figure 3 with the parameters k' and ϕ given in Table I. The solid lines in Figure 3 were determined by using these parameters and eq 14.

Discussion

The results of the three models give surprisingly good agreement in quantum yields considering the assumptions and other factors involved in the analysis of the data. The greatest error probably arises from the pseudo-zero-order approach because of the scatter in the data, which made it difficult to accurately determine a slope at short reaction times. In the first-order approach no provision is made for the absorption of light by the product, although the fact that eq 11 fits the data reasonably well suggests that the variation in light absorption at 435.8 nm is not a serious problem.

These results demonstrate that the quantum yield for the photoaquation of $[\text{Rh}(\text{NH}_3)_5\text{I}]^{2+}$ in a hydrated NaH-Y zeolite is 15–20% of that observed in aqueous solution. Upon removal of part of the zeolite water, the quantum yield decreased even more. The role of the zeolite in decreasing the quantum yield may be understood in light of the theory proposed by Kelly and Endicott⁶ to explain the photoaquation reaction in water. The authors suggest that d-d excitation of $[\text{Rh}(\text{NH}_3)_5\text{I}]^{2+}$ results in a vibrationally excited state in which the trans NH_3

ligand is nearly dissociated. The zeolite may provide a pathway for removal of this vibrational energy, or more likely the semirigid nature of the water molecules¹⁵ and the position of the complex in the zeolite may inhibit the replacement of the excited NH_3 ligand by H_2O . The effect of partial dehydration on quantum yield would favor the latter concept since the probability of having a water molecule in proper configuration for ligand exchange would be decreased. In this respect it is also important to note that, in the outer coordination sphere of the complex, the zeolite competes with water. Moreover, since the complex has the role of charge compensation for a negative zeolite lattice, it is expected that the favorable configuration of the complex would be along the wall of the large cavity with the chlorine extending into the large cavity and the trans ammonia ligand facing the lattice. In this geometric arrangement water would find it difficult to replace ammonia. Thus, steric factors may play an important role in the photochemical reaction.

The difficulty of carrying out photochemical reactions in a composite of highly scattering particles is also illustrated by this study. Transmission of visible light through these thin (ca. 40 μm) wafers was essentially zero, even when no absorber was present. Fluidization of powders has been suggested as a means of improving the efficiency of photochemical and photocatalytic reactions in solids; however, even if one started with very fine powders, agglomeration of particles would normally be a problem, resulting in inefficient utilization of light. A more reasonable alternative would be to carry out the processes in a medium with a refractive index similar to that of the solid so as to minimize the light-scattering problem.

Conclusions

The photochemical aquation of $[\text{Rh}^{\text{III}}(\text{NH}_3)_5\text{I}]^{3+}$ occurs within the cavities of a type-Y zeolite, but with a quantum yield that is only 15–20% of that observed in aqueous solution. This decrease in quantum yield is attributed to the decrease in mobility of water in the zeolite and to the exclusion of water from the ligand-exchange site by the zeolite lattice. Light scattering by the zeolite particles further reduces the efficiency of the photochemical reaction.

Acknowledgment. This work was partially supported by the National Science Foundation under Grant No. CHE-7706792 and the Robert A. Welch Foundation under Grant No. A-257.

Registry No. $[\text{Rh}(\text{NH}_3)_5\text{I}](\text{ClO}_4)_2$, 14282-98-5; NH_4^+ , 14798-03-9.

(14) Spencer, H. E.; Schmidt, M. W. *J. Phys. Chem.* **1970**, *74*, 3472.

(15) Shen, J. H.; Zettlemoyer, A. C.; Klier, K. *J. Phys. Chem.* **1980**, *84*, 1453.